Near-Cathode Plasma Layer on CuCr Contacts of Vacuum Arcs

Nelson A. Almeida, Mikhail S. Benilov, Larissa G. Benilova, Werner Hartmann, and Norbert Wenzel

***Abstract*— A model of near-cathode layers in vacuum arcs is developed. The model relies on a numerical solution of the problem of near-cathode space-charge sheath with ionization of atoms emitted by the cathode surface, and allows the self-consistent determination of all parameters of the near-cathode layer, including the ion backflow coefficient. The dependence of the density of energy flux from the plasma to the cathode surface on the local surface temperature is nonmonotonic with a maximum, a feature that plays an important role in the physics of plasma–cathode interaction. The developed model may be used for a variety of purposes, including as a module of complex nonstationary multidimensional numerical models of plasma–cathode interaction in vacuum arcs. As a simple example, an analytical evaluation of parameters of stationary spots on copper and chromium is given. In the case of composite** CuCr **contacts with large grains, spots with current of several tens of amperes burning on the copper matrix coexist with spots with currents of the order of 1 A burning on the chromium grains.**

***Index Terms*— Cathode spots, circuit breakers, composite cathodes, near-cathode plasma layers, vacuum arcs.**

I. Introduction

MAGNETOHYDRODYNAMIC (MHD) modeling of high-current arc discharges, both in ambient gas and in vacuum (or, more precisely, in cathode vapor), is an important research topic, which, in addition to being of scientific interest, is important due to numerous industrial applications of arc discharges. As far as arcs in ambient gas are concerned, such modeling has become a matter of routine (e.g., [1]–[11]), although a universally accepted model of plasma–cathode interaction in such discharges is still lacking (see discussion in [10]). Significant advances have been achieved also in the MHD modeling of vacuum arcs (e.g., [12]–[19] and references therein). However, the plasma–cathode interaction remains the element least understood, once again. One of the questions that remains open is the effect produced over plasma–cathode interaction in vacuum arcs by a granular structure of the cathode, an effect which is of significant interest since contacts of high-power vacuum circuit breakers are usually made of a composite material comprising different metals.

Some models of plasma–cathode interaction do not take into account specific phenomena localized near the cathode surface, such as separation of charges. As far as arcs in ambient gas are concerned, examples can be found in [1], [2], and [5]–[9], which employ the assumption of quasi-neutrality, or even the stronger assumption of local thermodynamic equilibrium, in the whole arc volume down to the cathode surface. As far as vacuum arcs are concerned, examples include [20]–[22], where a continuous metal–plasma transition without an interface is assumed. However, in most models of plasma–cathode interaction, specific phenomena localized near the cathode surface are of central importance, and in the first place separation of charges occurring in a very thin sheath adjacent to the cathode surface; see, review [23] and references therein and works [4], [10], [11], [24], [25] as far as arcs in ambient gas are concerned and [26]–[40] as far as vacuum arcs are concerned.

A direct 1-D modeling of near-cathode plasma layers has been performed with the use of diffusion equations [41] in the case of arcs in ambient gas and by means of Monte Carlo [42] and particle-in-cell [43]–[45] methods in the case of vacuum arcs. Neither of these approaches requires the near-cathode layer to be divided into subzones such as the space-charge sheath, the ionization layer, etc. However, these direct approaches are not suitable yet for serving as a module in self-consistent multidimensional calculation of arc attachments. Therefore, works dedicated to calculation of arc attachments employ less sophisticated models of near-cathode layers which are based on dividing the layer into subzones with the assumptions that there is no ionization in the near-cathode space-charge sheath and that the ion flux is formed in the quasi-neutral plasma beyond the sheath. The latter assumption is justified for arcs in ambient gas unless the gas pressure is very high [41]. As far as vacuum arcs are concerned, this assumption seems to be artificial [46, p. 106] and is disproved by estimates of characteristic length scales [47, Fig. 7.6], [48]. In other words, an accurate model of near-cathode layers in vacuum arcs should take into account the fact that the ionization of atoms emitted by the cathode surface occurs in the space-charge sheath. A qualitative treatment of such sheaths was given in [49], [50], and a self-consistent numerical solution was obtained in [51].

The aim of this paper is to develop, with the use of numerical results [51], a model of near-cathode layers in

Manuscript received December 14, 2012; accepted March 26, 2013. Date of publication June 13, 2013; date of current version August 7, 2013. This work was supported in part by Fundação para a Ciência e a Tecnologia of Portugal under Project PTDC/FIS-PLA/2708/2012 Modelling, understanding, and controlling self-organization phenomena in plasma-electrode interaction in gas discharges: from first principles to applications and Project PEst-OE/MAT/UI0219/2011 Centro de Ciências Matemáticas, and Siemens AG.

N. A. Almeida, M. S. Benilov, and L. G. Benilova are with the Departamento de Física, CCCEE, Universidade da Madeira, Funchal 9000, Portugal (e-mail: nelson@uma.pt; benilov@uma.pt; larissa@uma.pt).

W. Hartmann and N. Wenzel are with Siemens AG, Corporate Technology, Erlangen 91058, Germany (e-mail: werner.hartmann@siemens.com; norbert.wenzel@siemens.com).

Color versions of one or more of the figures in this paper are available online at http://ieeexplore.ieee.org.

Digital Object Identifier 10.1109/TPS.2013.2260832

vacuum arcs with cathodes made of a copper–chromium composite (chromium grains with characteristic dimensions from 10 to 50 μm, in a copper matrix). Since the characteristic thickness of the space-charge sheath, being far below 1 μm, is much smaller than the grain dimensions, it is legitimate to treat near-cathode layers on Cu and Cr separately and in the 1-D approximation. In the framework of this approach, all parameters of the near-cathode plasma should be determined as functions of the local surface temperature T_w and the near-cathode voltage drop U, similar to the way it is done for arcs in ambient gas, e.g., [23] and references therein.

A very important quantity to be delivered by a model of near-cathode layer of an arc discharge is the density of the net energy flux from the plasma to the cathode surface, $q = q\,(T_w, U)$. A characteristic feature of this quantity in the case of arcs in ambient gas is that its dependence on T_w for fixed U is nonmonotonic with a maximum (or two maxima), e.g., [23], fig. 6(a). It is this feature that, on one hand, gives rise to the instability leading to appearance of cathode spots and, on the other, makes possible the existence of stationary spots [52]. A similar character of the dependence of q on T_w for vacuum arcs was established in [31]. However, the model of near-cathode layers of vacuum arcs employed in [31] was elementary. On the other hand, a nonmonotonic with a maximum dependence $q\,(T_w)$ for fixed U has not apparently been reported in other works. This is one of the questions dealt with in this paper.

The model developed in this paper can be used for self-consistent 2-D or 3-D modeling of spots on CuCr vacuum arc cathodes. As the first step, results on stationary spots on large grains obtained by means of a simple analytical model [53], [54] are reported in this paper. Results on stationary and transient spots on grains of different sizes obtained by means of 2-D modeling are reported in [55] and in a forthcoming paper.

The outline of the paper is as follows: A model of near-cathode plasma layer in vacuum arcs is formulated in Section II. Results of evaluation of this model for copper and chromium cathodes are given in Section III. In Section IV, these results are integrated into an analytical model of stationary cathode spots and this model is used to qualitatively analyze spots on composite CuCr cathodes with large grains. Conclusions are summarized in Section V.

II. Equations of Near-Cathode Plasma Layer in Vacuum Arcs

The distribution of electrostatic potential in a near-cathode space-charge sheath with ionization of atoms emitted by the cathode surface possesses a maximum inside the sheath [49]–[51], as sketched in Fig. 1. The mechanism of formation of this potential hump may be described in brief as follows (see [51] for details): Since the ions coming to the cathode have been generated at rest inside the sheath, the electrostatic shielding is stronger than in a similar sheath with the ions having entered the sheath from the quasi-neutral plasma with the Bohm velocity. The electric field decays faster and vanishes at a finite distance from the cathode, which means a

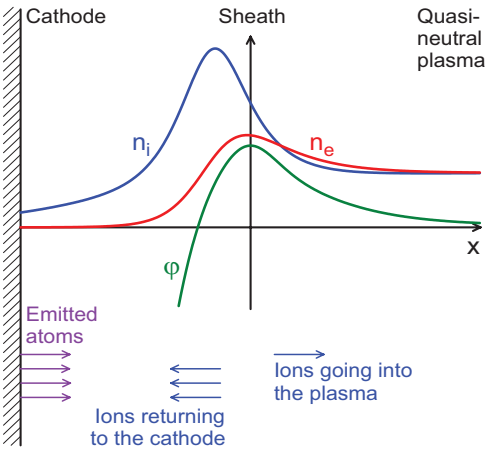

Fig. 1. Schematic of double sheath with ionization of emitted atoms. Reprinted from [51] with permission of IOP Publishing.

maximum of potential with subsequent reversal of the field. As the atoms emitted by the cathode move across the sheath, some of them get ionized before the potential maximum and others get ionized after the maximum. The ions produced before the maximum return to the cathode, and those produced after the maximum escape into the plasma. In either case, the ions suffer no collisions in the sheath, in particular, no charge exchange and no recombination. The physics of such sheaths is governed by two dimensionless parameters. One of these parameters is the dimensionless sheath voltage $\chi = eU/kT_e$ (here T_e is the temperature of thermalized electrons in the sheath, which is assumed to be constant across the sheath, and U is the sheath voltage). The other governing parameter characterizes the ratio of Debye and ionization lengths. In [51], this parameter is defined as

$$\alpha_w = \frac{v_a}{v_s}\frac{\varepsilon_0 kT_e}{n_{aw}e^2}\left(\frac{k_i n_{aw}}{v_a}\right)^2. \tag{1}$$

Here, $v_s = \sqrt{kT_e/m_i}$ is the Bohm speed, v_a is the average normal velocity of atoms emitted by the cathode surface, n_{aw} is the value of the density of the emitted atoms at the cathode surface, k_i is the rate constant of ionization of neutral atoms by electron impact (a function of T_e), and m_i is the mass of an atom.

The integral characteristics of the sheath relevant for calculation of plasma–cathode interaction that have been defined and computed in [51] are the following: τ is the ratio of characteristic fluxes of the atoms and the ions; Φ_∞ is the dimensionless potential difference between the sheath edge and the maximum; N_{aw} is the ratio of the atomic density at the cathode surface to the atomic density at the potential maximum; and Ψ_{iw}, $\Psi_{i\infty}$ are the dimensionless average potential energies with which ions are produced before and after the potential maximum, respectively. These parameters have been defined in a way that their dependence on the dimensionless sheath voltage χ is weak under conditions of practical interest, so one can consider these parameters as functions of a single control parameter α_w. In this paper, these functions are evaluated by means of the following fit formulas, which have been constructed on the basis of the numerical data

shown in [51, Fig. 6] converted to the argument α_w:

$$\tau = 0.48, \quad \Phi_\infty = -0.84 - \frac{0.42\alpha_w^{3/2}}{(\alpha_w + 5)\left(\sqrt{\alpha_w} + 3\right)} \tag{2}$$

$$N_{aw} = \frac{4}{1 + 0.8\sqrt{\alpha_w}} - 2 + 3.8\alpha_w^{1/3} \tag{3}$$

$$\Psi_{iw} = -\frac{0.5 + 0.3\sqrt{\alpha_w}}{1 + 0.3\sqrt{\alpha_w}}, \quad \Psi_{i\infty} = -\frac{0.3}{1 + (\alpha_w + 1)^{1/3}}. \tag{4}$$

With the use of these dependences, equations governing near-cathode layers in vacuum arcs may be written as follows. The density of electric current at the cathode surface is evaluated as $j = j_{iw} + j_{em} - j_{pl}$, where the terms on the rhs represent densities of, respectively, current of ions coming to the cathode surface (or, in other words, current of ions generated before the potential maximum), current of electrons emitted by the cathode surface, and current of thermalized electrons that come to the cathode from the sheath after having overcome the potential barrier.

The density of ion current may be evaluated as [51]

$$j_{iw} = \left(1 - N_{aw}^{-1}\right) e J_v \tag{5}$$

where $J_v = n_{aw} v_a$ is the number density of flux of the emitted atoms and the factor $\left(1 - N_{aw}^{-1}\right)$ has the meaning of the so-called ion backflow coefficient.

The electric field at the cathode surface, involved in the evaluation of the electron emission current density j_{em}, is governed by [51, Eq. (20)], which in dimensional form may be written as

$$E_w = \frac{kT_e}{e}\frac{k_i n_{aw}}{v_s}\sqrt{\frac{2}{N_{aw}\alpha_w}} \left\{(N_{aw} - 1)\sqrt{2(\chi - \Phi_\infty)}\left[1 + \frac{\Psi_{iw}}{2(\chi - \Phi_\infty)}\right] - \frac{1}{\tau}\right\}^{1/2}. \tag{6}$$

Since the sheath voltage constitutes at least several kT_e/e, only a small fraction of thermalized electrons reach the cathode surface, and the density of thermalized electrons inside the sheath is related to the electrostatic potential through the Boltzmann distribution. The current density of thermalized electrons reaching the cathode surface may be written as

$$j_{pl} = \frac{e}{4}\frac{J_v \exp\Phi_\infty}{N_{aw}\tau v_s}\sqrt{\frac{8kT_e}{\pi m_e}}\exp\left(-\frac{eU}{kT_e}\right). \tag{7}$$

Note that the second multiplier on the rhs has the meaning of the density of charged particles at the sheath edge.

Let us proceed to the equation of balance of electron energy in the sheath. Sources of the electron energy in the sheath are W_1, which is the energy brought in the sheath by emitted electrons, and W_2, which is the work of the electric field over the electrons inside the sheath. The energy brought in the sheath by the emitted electrons may be estimated as $W_1 = 2kT_w j_{em}/e$, where T_w is the local temperature of the cathode surface. (Note that the factor $2kT_w$ appears in place of $3kT_w/2$, which is what one would intuitively expect, because of the difference between the average value of the product of the kinetic energy of motion of electrons times the electron particle velocity, and the product of average values.) Work done by the electric field over the electrons inside the sheath is given by

$$W_2 = -\int_0^\infty j_e \frac{d\varphi}{dx} dx \tag{8}$$

where the coordinate x is measured from the cathode surface to the plasma, j_e is the projection along x-axis of the density of net electron current, and φ is the potential. Integrating by parts, setting $\varphi|_{x=\infty} = 0$, and taking into account that $\varphi|_{x=0} = -U$, one finds

$$W_2 = -\, j_e|_{x=0}\, U + \int_0^\infty \varphi \frac{dj_e}{dx} dx. \tag{9}$$

Taking into account the electron conservation equation $dj_e/dx = -e\omega$, where ω is the ionization rate, and the equality $j_e|_{x=0} = -j_{em} + j_{pl}$, one obtains

$$W_2 = \left(j_{em} - j_{pl}\right) U - \int_{-d}^\infty we\varphi\, dx. \tag{10}$$

The integral on the rhs may be expressed in terms of the dimensionless coefficients Ψ_{iw} and $\Psi_{i\infty}$. One finds finally

$$W_2 = \left(j_{em} - j_{pl}\right) U + kT_e \left[\frac{j_{iw}}{e}\left(\Psi_{i\infty} - \Psi_{iw}\right) - J_v\left(\Psi_{i\infty} - \Phi_\infty\right)\right]. \tag{11}$$

Sinks of the electron energy in the sheath are W_3, which is the energy carried away by thermalized electrons leaving the sheath for the cathode; W_4, which is the energy carried away by electrons leaving the sheath for the quasi-neutral plasma; and W_5, which is the electron energy lost inside the sheath for ionization. Applying Griem's criterion (e.g., [56] and references therein), one finds, for $T_e = 1$ eV, values of the electron density equal to 2×10^{21} m^{-3} for Cu and 9×10^{20} m^{-3} for Cr. Both values are by several orders of magnitude lower than characteristic electron densities in near-cathode layers of vacuum arcs. Hence, the rate of spontaneous radiative decay of excited states is by several orders of magnitude lower than the rates of collisional processes. For this reason, the electron energy lost inside the sheath for radiation is neglected.

The energy carried away by thermalized electrons going to the cathode is estimated as $W_3 = 2kT_e\frac{j_{pl}}{e}$. The energy carried away by electrons leaving the sheath for the plasma is estimated as

$$W_4 = 3.2kT_e\left(\frac{j}{e} + J_v - \frac{j_{iw}}{e}\right) \tag{12}$$

where the quantity in the parentheses on the rhs represents the flux of electrons leaving the sheath for the bulk plasma (note that $J_v - j_{iw}/e$ has the meaning of the density of the flux of ions leaving the sheath for the bulk plasma), and the factor 3.2 represents the sum of the coefficient $5/2$ accounting for enthalpy transport due to the electric current and of a thermal diffusion coefficient equal to 0.703. (The latter value

corresponds to the limiting case of a strongly to fully ionized plasma (e.g., [57, p. 410]). Finally, the losses of electron energy for ionization inside the sheath are $W_5 = J_v A_i$, where A_i is the ionization potential.

The resulting equation of balance of electron energy is written as

$$j_{em}\frac{2kT_w}{e} + \left(j_{em} - j_{pl}\right)U + \left[j_{iw}\left(\Psi_{i\infty} - \Psi_{iw}\right) - eJ_v\left(\Psi_{i\infty} - \Phi_\infty\right)\right]\frac{kT_e}{e} = j_{pl}\frac{2kT_e}{e} + \left(j + eJ_v - j_{iw}\right)\frac{3.2kT_e}{e} + J_v A_i. \quad (13)$$

Two comments should be made on this equation. First, the term W_4 is written under the assumption that the emitted electrons are thermalized in the sheath. In order to verify this assumption, one should compare δ, which is the scale of thickness of the sheath, with λ_{bt}, which is the length of relaxation of the beam of the emitted electrons. The scale of thickness of a collisionless near-cathode space charge may be estimated as [58]

$$\delta = \lambda_D\left(\frac{eU}{kT_e}\right)^{3/4}, \quad \lambda_D = \sqrt{\frac{\varepsilon_0 kT_e}{n_e e^2}} \quad (14)$$

where n_e is the density of thermalized electrons, and λ_D has the meaning of the Debye length. Assuming as representative values 20 bar for the pressure of thermalized electrons and 15 V for the sheath voltage U, one finds that δ increases from 0.016 μm for $T_e = 1$ eV to 0.029 μm for $T_e = 10$ eV.

The length of relaxation of the beam may be estimated as $\lambda_{bt} = 1/n_e Q_{bt}$, where Q_{bt} is the cross section of elastic collisions of the beam and thermalized electrons. The latter may be evaluated as (e.g., [57])

$$Q_{bt} = \frac{9\pi}{2}b_0^2 \ln\Lambda, \quad b_0 = \frac{e^2}{3\pi\,\varepsilon_0\varepsilon} \quad (15)$$

where ε is the energy of beam electrons and $\ln\Lambda = \ln(\lambda_D/b_0)$ is the Coulomb logarithm. Setting $T_e = 4$ eV, $n_e = 3 \times 10^{24}$ m^{-3} (which corresponds to the pressure of thermalized electrons of 20 bar), and $\varepsilon = 15$ eV, one finds $Q_{\rm bt} = 6 \times 10^{-19}$ m^2 and $\lambda_{bt} = 0.6$ μm. It follows that $\delta \ll \lambda_{bt}$ and the emitted electrons are thermalized in the quasi-neutral plasma beyond the sheath. Hence, (12) needs to be corrected: the energy carried away by electrons leaving the sheath for the bulk plasma should be evaluated separately for the thermalized electrons and the beam electrons, i.e., instead of (12) one should write

$$W_4 = \left(j + eJ_v - j_{iw} - j_{em}\right)\frac{3.2\,kT_e}{e} + j_{em}\left(\frac{2kT_w}{e} + U\right). \quad (16)$$

However, this is not the only correction that needs to be introduced into (12). Roughly speaking, the energy balance of electron gas in the near-cathode layers of vacuum arcs is as follows: the energy of emitted electrons accelerated in the space-charge sheath is transferred to thermalized electrons and subsequently spent for ionization of neutral atoms; and, if the transfer occurs (i.e., the emitted electrons get thermalized) in the quasi-neutral plasma beyond the sheath, i.e., beyond the zone where ionization occurs, then this energy must be transported by the thermalized electrons back into the sheath. This energy transport occurs through electron heat conduction, which is not taken into account in (16).

Thus, in order for (13) to correctly describe balance of the electron energy in the space-charge sheath, the second term on the rhs of this equation should be replaced by the rhs of (16) and supplemented by an account of heat conduction by thermalized electrons. However, (13), as it is, does represent a reasonable approximation for description of balance of the electron energy in a layer, which comprises both the space-charge sheath and the adjacent zone where the emitted electrons are thermalized. With this understanding, (13) is justified.

The second comment to be made on (13) is as follows: A part of the sheath voltage is applied not in the plasma but rather to the plasma/cathode interface, thus not contributing to acceleration/deceleration of the emitted/thermalized electrons but rather lowering the potential barrier between electrons in the cathode and in the plasma. Therefore, U in (13) should be replaced with $U_{\rm eff} = U - (A_f - A_{\rm eff})/e$, where A_f is the work function and $A_{\rm eff}$ is an "effective" work function.

In the framework of the above description, the physics of the near-cathode layer is governed by two control parameters, one of them being the temperature of the cathode surface at the point of the arc attachment being considered, and the other being an electric parameter, i.e., the local current density or the near-cathode voltage drop. It should be stressed that the absence of parameters characterizing the plasma ball is consistent with the physics considered: a significant power is deposited into the near-cathode layer; a part of this power is transported to the cathode and the rest is transported to the plasma ball. In other words, it is the near-cathode layer that heats the plasma ball and not the other way around.

Since the near-cathode voltage drop does not change much from one point of arc attachment to the other, the voltage drop makes a more convenient control parameter than the current density. Thus, control parameters used in this paper are T_w and U, similar to the usual procedure in the modeling of near-cathode phenomena in arcs in ambient gas; see, review [23] and references therein. If these parameters are specified, the above equations constitute a complete system. By solving this system for different values of T_w and U, one can determine all characteristics of the near-cathode layer as functions of T_w and U. (It should be emphasized that this is not equivalent to finding the distribution of characteristics in the arc attachment since T_w remains unknown until the arc attachment as a whole has been computed as is done, e.g., in [55]. Equally, one cannot establish a connection between U and the arc attachment current until the arc attachment as a whole has been computed.) In particular, the ion backflow coefficient (fraction of atoms emitted by the cathode surface that do not escape into the plasma but rather return to the cathode in the form of ions) may be found as $\mu = 1 - N_{aw}^{-1}$. The rate of ion erosion (loss of mass by the cathode due to emission of atoms per unit surface area and unit time) may be found as $G = N_{aw}^{-1} m_i J_v$. The density of the energy flux coming from the plasma to the

cathode surface may be found as

$$q = q_i - q_{ev} + q_e - q_{em} \tag{17}$$

$$q_i = \frac{j_{iw}}{e}\left[kT_e\left(\Psi_{iw} - \Phi_\infty\right) + eU_{\text{eff}} + A_i - A_{\text{eff}}\right],$$

$$q_{ev} = N_{aw}^{-1} J_v \left(A_v + 2kT_w\right) \tag{18}$$

$$q_e = \frac{j_{pl}}{e}\left(2kT_e + A_{\text{eff}}\right), q_{em} = \frac{j_{em}}{e}\left(2kT_w + A_{\text{eff}}\right) \tag{19}$$

where A_v is the vaporization energy per atom, and q_i, q_{ev}, q_e, and q_{em} represent, respectively, the density of the energy flux brought to the cathode surface by the incident ions, the net losses of energy of the cathode surface due to emission of atoms, heating of the cathode by thermalized electrons, and cooling (or heating) of the cathode due to electron emission. Heating of the cathode by radiation from the plasma is not taken into account. Note that the first and second terms in the square brackets on the rhs of the first equation in (18) represent the average kinetic energy of an incident ion, and the third and fourth terms represent the energy of neutralization.

It is useful to consider an alternative formula for the energy flux to the cathode surface, which is obtained by substituting (18) and (19) into (17) and subtracting (13) from the relationship obtained

$$q = jU - \frac{j}{e}\left(A_f + 3.2kT_e\right) - \frac{G}{m_i}\left[A_v + A_i + \left(3.2 + \Psi_{i\infty} - \Phi_\infty\right)kT_e + 2kT_w\right]. \tag{20}$$

This formula has a clear physical meaning: it describes the energy balance of the sheath (or, more precisely, of the layer comprising the space-charge sheath and the adjacent zone where the emitted electrons are thermalized). The first and second terms on the right-hand side are the same as in the corresponding expression for arcs in ambient gas [23, Eq. (11)] and represent, respectively, the electrical power deposited per unit area of the sheath and the energy transported from the sheath into the bulk plasma by the electric current, calculated taking into account the energy necessary for extracting electrons from the cathode. The third term represents the energy transported from the sheath into the bulk plasma by the flux of erosion products. The terms A_v and A_i in the square brackets describe the energy necessary for extracting neutral atoms from the cathode and ionizing them. The product $\left(\Psi_{i\infty} - \Phi_\infty\right)kT_e$ in the square brackets describes the kinetic energy of the ion jet leaving the sheath, and the term $2kT_w$ accounts for the thermal energy of the ion jet. Note that the last term is at best only approximately correct, since terms of the order of kT_w have been neglected in comparison with terms of the order of kT_e in the analysis of the sheath in [51].

The above model is based on the assumption that all the atoms emitted by the cathode surface are ionized inside the space-charge sheath, rather than in the quasi-neutral plasma beyond the sheath. This assumption is justified at high values of the electron temperatures T_e in the near-cathode layer, which are characteristic for the central part of the cathode spot; see, the estimates [48]. On the other hand, this assumption is hardly adequate for space-resolved modeling, which is aimed at investigating the whole structure of the spot, including its periphery: since T_e is low at the periphery, only a fraction of the atoms emitted by the cathode surface are ionized in the sheath and the rest are ionized in the quasi-neutral plasma beyond the sheath, where collisions may be essential.

In this paper, this is taken into account in a qualitative way. Let ω be the ionization degree evaluated according to the formula $\omega = n_e/\left(n_a + n_i\right)$ taking into account the doubly and triply charged ions for conditions of ionization equilibrium at the heavy-particle temperature T_w, the electron temperature T_e, and the plasma pressure equal to $n_{aw}kT_w$. (Here, n_a and n_i are atomic and ion densities. Note that ω defined in this way represents the conventional ionization degree under conditions where doubly and triply charged ions are absent; if the plasma is fully ionized, ω represents the average charge number of the ions.) If $\omega \geq 1$, it is assumed that all the atoms emitted by the cathode surface are ionized inside the space-charge sheath and the above model is used as it is. If $\omega < 1$, it is assumed that a part of atoms emitted by the cathode surface are ionized inside the sheath and the other part leave the sheath without being ionized and are ionized in the quasi-neutral plasma, and fractions of these parts are, respectively, ω and $1 - \omega$. In the framework of this approach, the following changes are required in the above formulas in the case $\omega < 1$: the density of atoms emitted by the cathode, n_{aw}, is replaced by ωn_{aw}; the number density of the erosion flux, which in the above model equals $n_{aw}v_a/N_{aw}$, is now evaluated as the sum of flux of atoms ionized inside the sheath but beyond the maximum of potential, $\omega n_{aw}v_a/N_{aw}$, and of the flux of atoms ionized in the quasi-neutral plasma, $(1-\omega)\,n_{aw}v_a$.

Finally, let us specify the material constants appearing in the above equations for cathode material being Cu or Cr, which is the case of concern for this paper. The flux of atoms emitted by the cathode surface is estimated by means of the Langmuir formula: $J_v = p_v/\sqrt{2\pi m_i kT_w}$, where p_v is the pressure of the saturated vapor of the cathode material at the temperature T_w. The pressure of the saturated vapor of Cu and Cr is estimated with the use of [59] and [60], respectively. The average normal velocity of atoms emitted by the cathode surface and the density of the emitted atoms at the cathode surface are estimated as $v_a = \sqrt{2kT_w/\pi m_i}$ and $n_{aw} = J_v/v_a$.

The electron emission current density j_{em} is evaluated in the framework of the Murphy and Good theory [61]. It is known that a computationally efficient and accurate evaluation of the Murphy and Good formulas is not trivial. Indeed, it was found that a straightforward numerical implementation of the Murphy and Good formulas results in significant errors in characteristics of the near-cathode layer and/or makes the code unreasonably slow. In this connection, a new method [62] was developed which relies on Padé approximants and is as simple and computationally efficient as possible while being accurate in the full range of conditions of validity of the Murphy and Good theory.

The effective work function A_{eff} is evaluated by means of fit formulas which have been derived in [63] on the basis of

the Murphy–Good formalism. (Note that A_{eff} is related to the average energy ε of an emitted electron, which was dealt with in [63], by the formula $\varepsilon = A_{\text{eff}} + 2kT_w$.)

The ionization rate constant is evaluated as the sum of the rate constant of direct ionization of atoms from the ground state and rate constant of stepwise ionization: $k_i = k_{\text{idir}} + k_{\text{ist}}$. k_{idir} is evaluated by means of the data [64] for chromium and by means of the formula from [65] with the use of data on the cross section of direct ionization of neutral atoms [66] for copper. k_{ist} is evaluated by means of the formula from [65]. Note that, under typical conditions of vacuum arcs, the stepwise ionization of both copper and chromium atoms occurs much faster than the direct ionization, i.e., $k_{\text{idir}} \ll k_{\text{ist}}$, which is a consequence of the presence of low-lying energy levels.

III. Parameters of Near-Cathode Plasma Layers on Copper and Chromium Cathodes

Let us consider the results of evaluation of the system of equations of near-cathode layers in vacuum arcs formulated in the preceding section for the case of copper and chromium cathodes. Because of the high electrical conductivity of the plasma, variations of potential on the plasma side of the sheath are much smaller than the near-cathode voltage U. Therefore, one can assume that the near-cathode voltage takes the same value at every point of the spot (the arc attachment). Then it is appropriate to present parameters of the near-cathode layer as functions of the local surface temperature T_w for fixed values of U. As an example, dependences of characteristics of the near-cathode layer on T_w calculated for a copper cathode and the near-cathode voltage of 20 V are shown in Fig. 2.

As the local surface temperature decreases, a transition to a regime without the plasma occurs. This transition manifests itself through not only a decrease in the evaporation flux but also a decrease in the electron temperature T_e and, consequently, the ionization degree ω of the plasma; for example, under conditions of Fig. 2, T_e and ω are equal to, respectively, 5479 K and 5.19×10^{-3} for $T_w = 3000$ K, and they continue to decrease for T_w still lower. Eventually the numerical calculations break down since in the course of iterations T_e becomes too low or even negative. It is natural to interpret this breakdown as an indication that a transition to a regime without the plasma has been completed and to switch to a no-plasma solution: the current density j is set equal to the electron thermionic emission current density and evaluated by means of the Richardson equation; the energy flux density q is set equal to the sum of thermionic and evaporation cooling; the erosion rate G is assumed to be governed by the evaporation (no return of ions, i.e., the ion backflow coefficient μ is set equal to zero) and evaluated by means of the Langmuir formula. Under conditions of Fig. 2, the switching from the plasma-present to no-plasma solutions occurs at T_w between 2370 and 2360 K (note that these data have been calculated with the step in T_w equal to 10 K). A magnification of Fig. 2(a) in the vicinity of the switching is shown in Fig. 3. The electron temperature, the ionization degree, and the ion backflow coefficient for $T_w = 2370$ K are already very low: $T_e = 3821$ K, $\omega = 5.4 \times 10^{-4}$, and $\mu = 2.7 \times 10^{-4}$, which

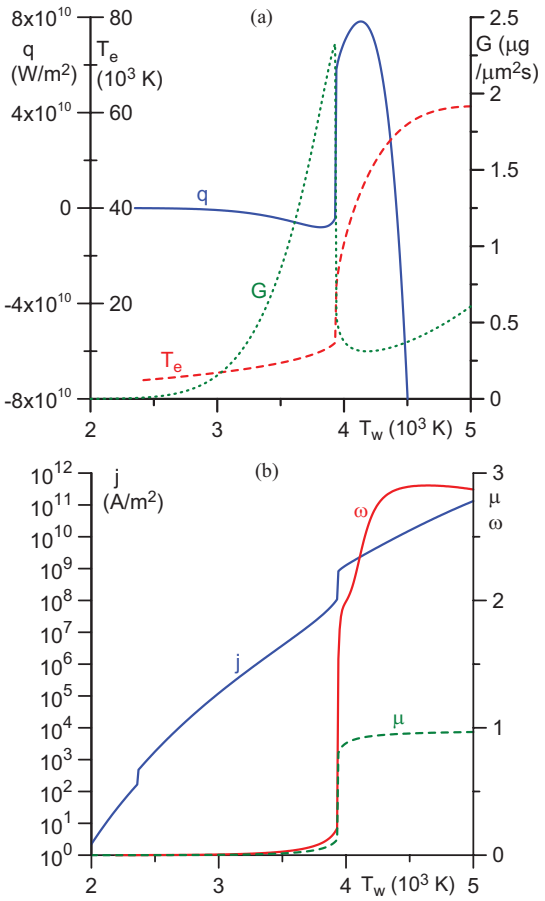

Fig. 2. Characteristics of near-cathode plasma layer versus cathode surface temperature. (a) Density of the energy flux from the plasma to the cathode surface, the erosion rate, and the electron temperature. (b) Density of the electric current, the ion backflow coefficient, and the ionization degree. Cu cathode, $U = 20$ V.

is why discontinuities in the energy flux from the plasma and the erosion rate, $q\,(T_w)$ and $G\,(T_w)$, are small and cannot be seen in Fig. 3. The discontinuity in the current density, $j\,(T_w)$, is visible in Fig. 2(b); however, the absolute values of j are very low here. Therefore, this discontinuity is irrelevant from the point of view of physics and does not pose a problem for computation of spots.

There is another discontinuity in the data shown in Fig. 2, which occurs at T_w between 3940 and 3930 K, i.e., slightly lower than the temperature corresponding to the maximum of the dependence $q\,(T_w)$, and is quite strong. This discontinuity is illustrated by Fig. 4. The calculations shown in this figure have been performed in two ways: in the direction from higher values of T_w to lower values, similar to the way it was done while calculating the data plotted in Figs. 2 and 3, and in the reverse direction. In both sets of calculations, the results obtained for the previous value of T_w have been used as an initial approximation for the current value. The step in T_w was 1 K. The calculation results are depicted by the solid lines and represent two disconnected branches; the switching from one branch to the other occurs as shown by arrows and is accompanied by hysteresis.

It is natural to assume that the two computed branches are in reality connected by a retrograde section, as schematically

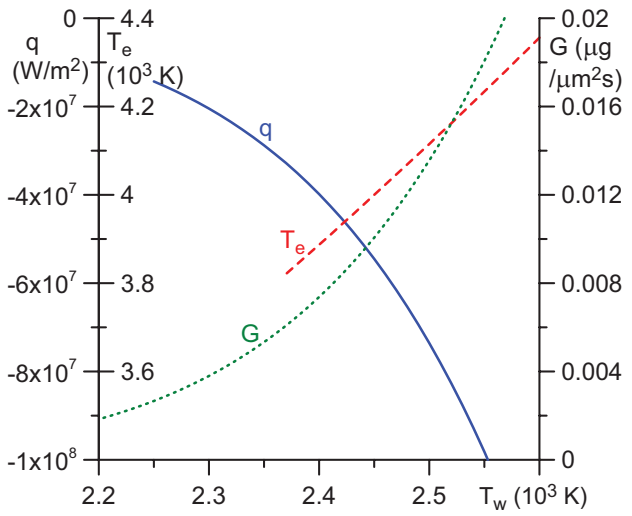

Fig. 3. Switching between the no-plasma and plasma-present solutions. Cu cathode, $U = 20$ V.

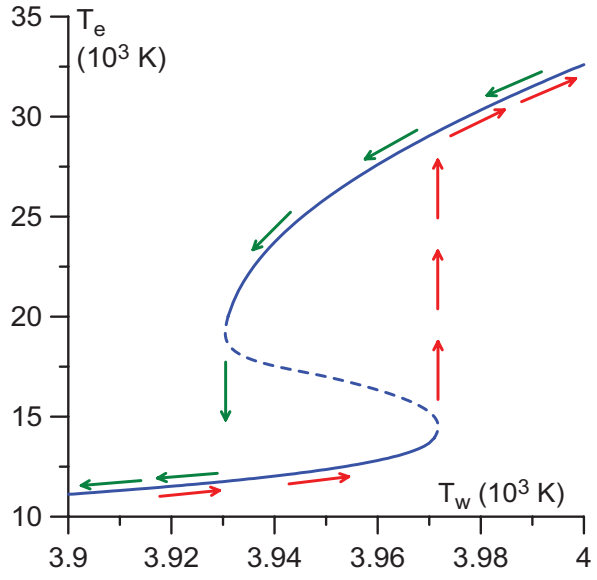

Fig. 4. Hysteresis in calculations of the near-cathode plasma layer. Cu cathode, $U = 20$ V.

shown in Fig. 4 by the dashed line. It would be interesting to compute this retrograde section and analyze the underlying physics. However, this section is localized in a narrow range of T_w and does not seem to be very important for the calculation of spots on the whole. Therefore, calculation of the retrograde section is left beyond the scope of this paper and the results are used that have been obtained by calculations in the direction of decreasing T_w, with the discontinuity in the dependence $q\,(T_w)$ being smoothed numerically.

One can see from Fig. 2(a) that the dependence of q on T_w is nonmonotonic with a maximum, which is in agreement with a similar result [31] obtained on the basis of an elementary model. This feature is characteristic also of near-cathode layers in arcs in ambient gas, e.g., [23, Fig. 6(a)]. The reason of the nonmonotonicity in the case of vacuum arcs is the same as in the case of arcs in ambient gas: as T_w increases, the ion heating of the cathode grows faster than the electron emission cooling at T_w below approximately 4130 K and vice versa at higher T_w. Note that heating of the cathode surface by thermalized electrons is a minor effect; the evaporation cooling prevails over all other mechanisms for lower temperatures where $q\,(T_w)$ is negative ($T_w \leq 3930$ K in the above conditions) and is insignificant for higher T_w.

The nonmonotonicity of the dependence of q on T_w plays a very important role in the theory of cathode spots in arcs in ambient gas [52]. The rising section of this dependence is potentially unstable: a local increase of the surface temperature will result in an increase of the local energy flux from the plasma; the latter will cause a new increase of the local temperature, etc, i.e., a thermal instability will develop, leading to the appearance of a cathode spot. On the other hand, stationary spots operate on the falling (i.e., stable) section of the dependence $q\,(T_w)$. Therefore, the nonmonotonicity of the dependence of q on T_w in the case of vacuum arcs suggests that spots on cathodes of vacuum arcs may appear as a result of instability of nonlinear surface heating of the cathode by the plasma and that stationary regimes of cathode spots in vacuum arcs are possible, at least in cases where the Joule heating inside the cathode is insignificant.

Although the dependences $q\,(T_w)$ in the cases of vacuum arcs and arcs in ambient gas are qualitatively similar, there is a significant quantitative difference: the maximum in this dependence in the case of vacuum arc is higher by more than two orders of magnitude and by about a factor of two more narrow.

While the function $q\,(T_w)$ is nonmonotonous, the function $j\,(T_w)$ is monotonically increasing, as can be seen from Fig. 2(b). The electron temperature T_e [Fig. 2(a)] increases with increasing T_w in the range $T_w \lesssim 4500$ K, which is a consequence of increasing input of electron energy into the sheath resulting from acceleration of emitted electrons by the sheath electric field. For higher T_w, the dependence $T_e\,(T_w)$ becomes saturated. The ion backflow coefficient μ [Fig. 2(b)] is very low for $T_w \lesssim 3930$ K; the plasma density is low, and virtually all vaporized atoms escape from the near-cathode sheath into the plasma without being ionized. μ is close to unity for higher T_w; most of the vaporized atoms get ionized before the potential maximum and return to the cathode. The erosion rate G [Fig. 2(a)] increases in the range $T_w \lesssim 3930$ K, passes through a maximum, and then starts decreasing. This is readily understandable if one takes into account that $G = (1-\mu)\,m_i\,J_v$. For $T_w \lesssim 3930$ K, the escape factor $1-\mu$ is close to unity while the dependence $J_v\,(T_w)$ increases, and so does the erosion rate. The escape factor rapidly decreases for T_w slightly above 3930 K, and so does the erosion rate. For higher temperatures, the erosion rate passes through a minimum and starts increasing once again.

Characteristics of the near-cathode layer on chromium cathodes for the near-cathode voltage of 20 V are shown in Fig. 5. The data shown in this figure are qualitatively similar to those for copper shown in Fig. 2. A quantitative comparison of the most important parameters, i.e., densities of energy flux and electric current from the plasma to the cathode surface, is shown in Fig. 6 for two values of the near-cathode voltage drop. One can see that these parameters are not very different quantitatively. The most important difference is that

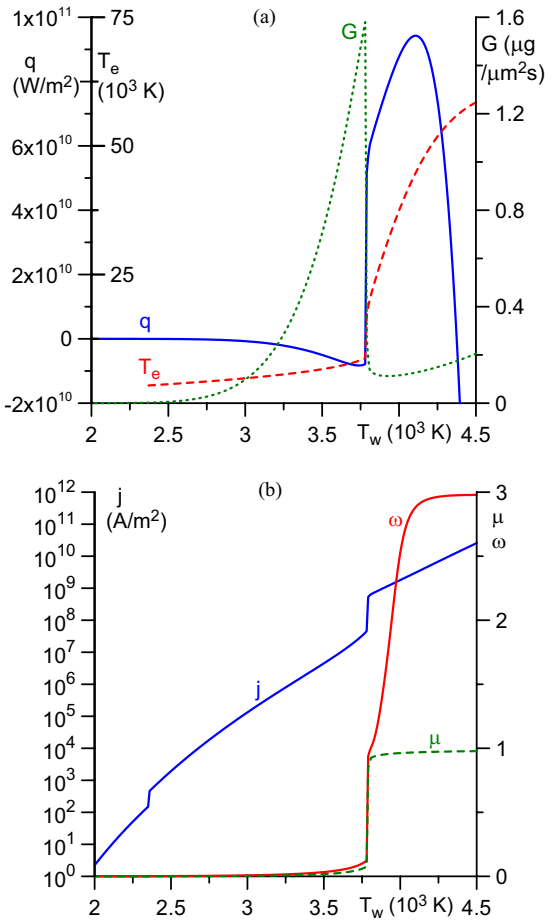

Fig. 5. Characteristics of the near-cathode plasma layer versus cathode surface temperature. Cr cathode, $U = 20$ V.

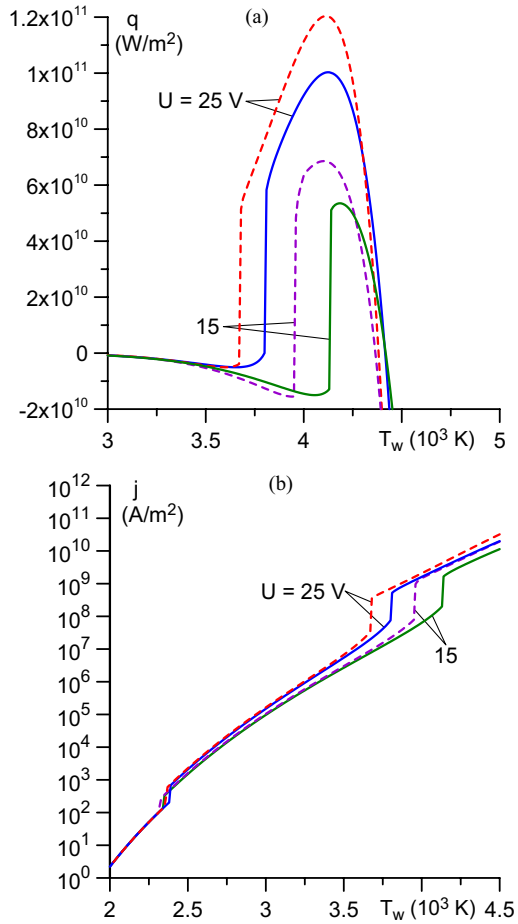

Fig. 6. Comparison of (a) the densities of energy flux and (b) electric current for Cu and Cr cathodes. Solid: Cu cathode. Dashed: Cr cathode.

the maximum in the dependence $q\,(T_w)$ is somewhat wider in the case of chromium.

IV. Analytical Model of Stationary Spots on Cathodes of Vacuum Arcs and Spots on Composite CuCr Cathodes With Large Grains

The model of near-cathode layers in vacuum arcs developed in Section II may be used for a variety of purposes, including as a module of complex nonstationary multidimensional numerical models of the plasma–cathode interaction. As a simple example, let us apply this model to the analytical investigation of stationary spots on copper and chromium with the aim to qualitatively analyze the spots on composite CuCr cathodes with large grains. Of course, an analytical approach has its limitations; however, it provides a useful insight which, as it will be shown in [55] and a forthcoming paper, is helpful in understanding results of complex space-resolved numerical modeling, both stationary and nonstationary.

Let us designate by T_* the value of the cathode temperature T_w at which the dependence $q\,(T_w)$ for a given U attains the maximum value. Let us designate by T_1 and T_2 values of T_w at which the dependence $q\,(T_w)$ vanishes, with T_1 belonging to the growing branch of the dependence $q\,(T_w)$ and T_2 to the falling branch, so that $T_1 < T_* < T_2$. For $T_w > T_2$, the electron emission cooling exceeds the ion heating and the energy flux is directed from the cathode into the plasma, $q < 0$.

If Joule heating in the cathode body is insignificant, then the temperature at any point of the cathode inside a stationary arc attachment cannot exceed the value T_2 [52]. This is an exact result that follows from the maximum principle for harmonic functions and also from intuitive considerations: values of the temperature exceeding T_2 cannot be maintained since heat flux originating in points of the surface where the energy flux from the plasma is positive (and, consequently, $T_w < T_2$) cannot propagate from these points to a hotter point. Furthermore, $|q\,(T_w)|$ increases extremely rapidly for $T_w > T_2$, hence the temperature of the cathode surface cannot appreciably exceed T_2 even if Joule heating in the cathode body does play a role.

Stationary spots on large cathodes operate on the falling section of the dependence $q\,(T_w)$: the temperature inside the spot varies from T_* at the spot edge to a somewhat higher value at the center of the spot, the latter value being close to T_2. This follows from numerical calculations [31], [52] and is intuitively clear: a stationary spot cannot operate on the rising section of the dependence $q\,(T_w)$, which is prone to thermal instability.

Let us designate by T_∞ the temperature of the cathode far away from the spot. The ratio $(T_2 - T_1)\,/\,(T_2 - T_\infty)$ represents the relative width of the maximum of the dependence

$q\,(T_w)$. Let us treat this ratio as a small parameter; one can see from Figs. 2(a), 5(a), and 6(a) that this approximation is not unreasonable. Furthermore, let us neglect values of the function $q\,(T_w)$ in the range $T_w < T_1$ and limit the consideration to conditions where Joule heating in the cathode body is insignificant. Then one can use the analytical model of the stationary cathode arc spot [53], [54]. It should be stressed that this model does not involve empirical parameters and/or arbitrary theoretical assumptions; rather, it represents an asymptotic form of a detailed model of stationary arc spots (which can be dealt with only numerically) and is in this sense mathematically solid. In the framework of this model, the radius of a spot may be estimated as [53]

$$R = \frac{\psi_*^2}{\pi}\left[\int_{T_1}^{T_2} q\,(T_w, U)\;\kappa\,(T_w)\;\,dT_w\right]^{-1}. \qquad (21)$$

Here, κ is thermal conductivity of the cathode material (function of the local temperature) and ψ_* is the heat flux potential, $\psi_* = \int_{T_\infty}^{T_*} \kappa\,(T_w)\;dT_w$. The power coming from the plasma to the spot is given by the formula $Q_p = 4R\psi_*$, which follows from a solution of the heat conduction equation in a half-space heated by a circle with a constant temperature [67, Ch. VIII, Sec. 2].

Integrating (20) over the spot, one obtains the following expression for the so-called heating voltage $U_h = Q_p/I$, where I is current per spot:

$$U_h = U - \frac{1}{e}\left(A_f + 3.2k\bar{T}_e\right) - \frac{\bar{g}}{m_i}\left[A_v + A_i + \left(3.2 + \bar{\Psi}_{i\infty} - \bar{\Phi}_\infty\right)k\bar{T}_e + 2k\bar{T}_w\right] \qquad (22)$$

where $g = G/j$ is the so-called g-factor (the loss of mass of the cathode per unit charge transported) and the bar designates the weighted average values of the corresponding quantities evaluated over the spot.

A simple approximation appropriate in the framework of the analytical model being considered is to set the average values equal to the corresponding values for $T_w = T_*$, i.e., at the point of maximum of the dependence $q\,(T_w)$ for given U. In terms of the physics involved, this amounts to setting average values equal to values of the corresponding quantities at the edge of the spot.

Formulas (21) and (22) allow one to estimate all parameters of a stationary cathode spot for a given near-cathode voltage drop U provided that the characteristics of the near-cathode plasma layer for this U have been computed. Current–voltage characteristics of spots on copper cathodes for three values of the temperature of the cathode surface outside spots are shown in Fig. 7(a). Also shown are the g-factor and the parameter α_w (both evaluated for $T_w = T_*$). One can see that U decreases with increasing I and T_∞; however, both dependences are weak. Roughly speaking, for the spot current of several tens of amperes, U is around 15−20 V. (For example, for $I = 50$ A, the voltage drop is 19.5 V for $T_\infty = 500$ K, 16 V for $T_\infty = 1000$ K, and 14 V for $T_\infty = 1500$ K). The g-factor is within the range 12–32 μgC^{-1}. (The g-factor in this paper refers to the erosion due to the flux of ions leaving the near-cathode layer for the bulk plasma; the erosion due to formation of macroparticles is not considered. Note that experimental values of ion erosion rate for copper are in the range 33–39 μg/C [46, p. 157].) The temperature at the spot edge, T_*, varies from 4180 to 4130 K; note that these values correspond to $U = 15$ V and $U = 20$ V, respectively. The maximum temperature at the center of the spot, T_2, is 4420 K (for all U from the range considered). The spot radius varies between approximately 25 and 70 μm for I in the current range from 20 to 80 A, the electron temperature in the near-cathode layer is between 2 and 4 eV, and the electric field at the cathode surface is around 2.4×10^9 Vm^{-1}. While these values are not intended for a quantitative comparison with the experiment, it is worth noting that they fit into the usual range of parameters of macrospots, or group spots; e.g., review [68]. Parameter α_w is much larger than unity, which is an indication that ionization of evaporated atoms inside the spot occurs mostly in the space-charge sheath.

Results of calculations of spots on chromium cathodes are shown in Fig. 7(b). One can see that comparable values of the near-cathode voltage drop occur on chromium cathodes for significantly lower currents than those on copper cathodes. The radius of spots on chromium is 3–11 μm, the g-factor is 4–7 μgC^{-1}, the electron temperature in the near-cathode layer and the electric field at the cathode surface are similar to those for copper, and the parameter $\alpha_{\rm w}$ is still bigger than for copper.

The above-described significant difference in the spot current and radius of spots on copper and chromium, which has been found by means of an approximate analytical treatment, is confirmed by an accurate 2-D modeling of stationary spots [55]. A detailed analysis of this difference is given in [55]; here we only note that it is due in the first place to a significantly higher thermal conductivity of copper.

The above results on individual spots may be used for qualitative analysis of spots on contacts made of composite CuCr material in the case where the chromium grains are large, say of characteristic dimensions of 20 μm or higher. Then there are independent spots burning on the copper matrix and the chromium grains, and these spots operate in parallel, i.e., at the same value of the near-cathode voltage. The current per spot on copper is of several tens of amperes, and that on chromium is of the order of one or a few amperes. If one assumes that the distribution of spots over the electrode surface (i.e., the number of spots per unit area of the surface of the contact) does not vary much from copper to chromium, then the ratio of ion erosion rates of chromium and copper surfaces may be estimated as $G_{\rm Cr}/G_{\rm Cu} = I_{\rm Cr}g_{\rm Cr}/I_{\rm Cu}g_{\rm Cu}$, where $I_{\rm Cr}$, $g_{\rm Cr}$, and $I_{\rm Cu}$, $g_{\rm Cu}$ are current per spot and g-factor of spots on chromium and copper, respectively. One can see from Fig. 7 that $I_{\rm Cr}g_{\rm Cr}/I_{\rm Cu}g_{\rm Cu}$ is of order of 10^{-2}. Hence, $G_{\rm Cu}$, which is the rate of ion erosion of copper per unit surface area and unit time, exceeds $G_{\rm Cr}$, which is the rate of erosion of chromium, by two orders of magnitude. Note that these conclusions conform to results of space-resolved numerical modeling [55].

It should be noted that, because of the low current, small diameter, and low erosion rate, spots on chromium should be

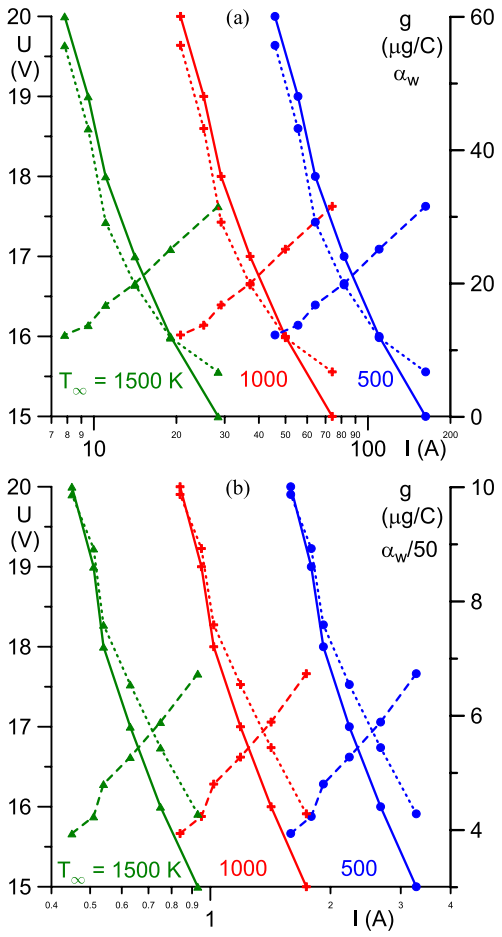

Fig. 7. Current–voltage characteristics (solid), g-factor (dashed), and parameter α_w (dotted). (a) Cu cathodes. (b) Cr cathodes.

much dimmer than those on copper. Hence, it is likely that the spots on chromium are overlooked in many experiments on composite cathodes. On the other hand, high-resolution photographs of high-current arcs between copper-chromium contacts taken at exposure times of 2 μs [69]–[71] revealed cathode spots with the average current of 45 A similar to those on pure copper cathodes, as well as very small and dim spots. It is legitimate to identify the small spots with the spots on chromium, as predicted by the above theoretical treatment.

V. Conclusion

A model of near-cathode layers in vacuum arcs has been developed. The model relies on a numerical solution of the problem of near-cathode space-charge sheath with ionization of atoms emitted by the cathode surface. It allows the self-consistent determination of all parameters of the near-cathode layer, including the ion backflow coefficient, as functions of the local surface temperature T_w and the near-cathode voltage drop U. Evaluation results were given for copper and chromium cathodes.

The dependence of the density of energy flux from the plasma to the cathode surface on T_w was shown to be non-monotonic with a maximum, in agreement with the previous result [31]. This feature stems from the fact that the ion heating of the cathode grows faster than the electron emission cooling at lower T_w, and vice versa at higher T_w. It is characteristic also of near-cathode layers in arcs in ambient gas. This feature is very important theoretically and suggests that spots on cathodes of vacuum arcs may appear as a result of thermal instability developing in the cathode body and that stationary regimes of cathode spots in vacuum arcs are possible as far as thermal instability is concerned, similar to what happens in the theory of cathode spots in arcs in ambient gas.

The developed model of near-cathode layers in vacuum arcs may be used for a variety of purposes, including as a module of complex nonstationary 2-D and 3-D numerical models of plasma–cathode interactions. As a simple example, an analytical evaluation of parameters of stationary spots on copper and chromium was performed in this paper. Of course, the analytical approach has its limitations and is not intended for a quantitative comparison with the experiment; however, it provides a useful insight which, as it will be shown in [55] and a forthcoming paper, is helpful in understanding results of complex 2D numerical modeling, both stationary and non-stationary. Spot parameters given by this model fit in the range of parameters of macrospots available in the literature.

Results of investigation of individual spots on copper and chromium may be used for qualitative analysis of spots on contacts made of composite CuCr material in the case where the chromium grains are large. There are spots with currents of several tens of amperes burning on the copper matrix, which coexist with spots with currents of the order of one or a few amperes burning on the chromium grains. The rate of ion erosion of copper per unit area and unit time exceeds the rate of erosion of chromium by two orders of magnitude. It should be emphasized that these conclusions conform to results of space-resolved numerical modeling [55].

References

[1] A. Gleizes, J. J. Gonzalez, and P. Freton, "Thermal plasma modelling," *J. Phys. D, Appl. Phys.*, vol. 38, no. 9, pp. R153–R183, May 2005.

[2] J. J. Lowke and M. Tanaka, "'LTE-diffusion approximation' for arc calculations," *J. Phys. D, Appl. Phys.*, vol. 39, no. 16, pp. 3634–3643, Aug. 2006.

[3] H.-P. Li and M. S. Benilov, "Effect of a near-cathode sheath on heat transfer in high-pressure arc plasmas," *J. Phys. D, Appl. Phys.*, vol. 40, no. 7, pp. 2010–2017, Apr. 2007.

[4] J. J. Gonzalez, F. Cayla, P. Freton, and P. Teulet, "Two-dimensional self-consistent modelling of the arc/cathode interaction," *J. Phys. D, Appl. Phys.*, vol. 42, no. 14, pp. 145204-1–145204-3, Jul. 2009.

[5] M. Schnick, U. Fuessel, M. Hertel, M. Haessler, A. Spille-Kohoff, and A. B. Murphy, "Modelling of gas–metal arc welding taking into account metal vapour," *J. Phys. D, Appl. Phys.*, vol. 43, no. 43, pp. 434008-1–434008-4, Nov. 2010.

[6] A. B. Murphy, "A self-consistent three-dimensional model of the arc, electrode and weld pool in gas–metal arc welding," *J. Phys. D, Appl. Phys.*, vol. 44, no. 19, pp. 194009-1–194009-6, May 2011.

[7] Y. Ogino, Y. Hirata, and K. Nomura, "Numerical analysis of the heat source characteristics of a two-electrode TIG arc," *J. Phys. D, Appl. Phys.*, vol. 44, no. 21, pp. 215202-1–215202-2, Jun. 2011.

[8] V. Colombo, E. Ghedini, M. Boselli, P. Sanibondi, and A. Concetti, "3D static and time-dependent modelling of a DC transferred arc twin torch system," *J. Phys. D, Appl. Phys.*, vol. 44, no. 19, pp. 194005-1–194005-9, May 2011.

[9] A. Lebouvier, C. Delalondre, F. Fresnet, F. Cauneau, and L. Fulcheri, "3D MHD modelling of low current–high voltage DC plasma torch under restrike mode," *J. Phys. D, Appl. Phys.*, vol. 45, no. 2, pp. 025203–025204, Jan. 2012.

[10] M. S. Benilov, L. G. Benilova, H.-P. Li, and G.-Q. Wu, "Sheath and arc-column voltages in high-pressure arc discharges," *J. Phys. D, Appl. Phys.*, vol. 45, no. 35, pp. 355201-1–355201-2, Sep. 2012.

[11] M. Baeva, R. Kozakov, S. Gorchakov, and D. Uhrlandt, "Two-temperature chemically non-equilibrium modelling of transferred arcs," *Plasma Sour. Sci. Technol.*, vol. 21, no. 5, pp. 055027-1–055027-9, Oct. 2012.

[12] M. Keidar, I. Beilis, R. L. Boxman, and S. Goldsmith, "2D expansion of the low-density interelectrode vacuum arc plasma jet in an axial magnetic field," *J. Phys. D, Appl. Phys.*, vol. 29, no. 7, pp. 1973–1983, Jul. 1996.

[13] E. Schade and D. L. Shmelev, "Numerical simulation of high-current vacuum arcs with an external axial magnetic field," *IEEE Trans. Plasma Sci.*, vol. 31, no. 5, pp. 890–901, Oct. 2003.

[14] M. Keidar, M. B. Schulman, and E. D. Taylor, "Model of a diffuse column vacuum arc with cathode jets burning in parallel with a high-current plasma column," *IEEE Trans. Plasma Sci.*, vol. 32, no. 2, pp. 783–791, Apr. 2004.

[15] Ya. I. Londer and K. N. Ul'yanov, "A two-dimensional mathematical model of a short vacuum arc in external magnetic field: Results of numerical calculations," *High Temp.*, vol. 44, no. 1, pp. 22–28, Jan. 2006.

[16] W. Hartmann, A. Hauser, A. Lawall, R. Renz, and N. Wenzel, "Development of a FEM simulation of axial magnetic field vacuum arcs," in *Proc. 23rd Int. Symp. Discharges Electr. Insul. Vacuum*, vol. 2. Sep. 2008, pp. 398–401.

[17] Y. Langlois, P. Chapelle, A. Jardy, and F. Gentils, "On the modeling of a diffuse vacuum arc in the presence of an axial magnetic field," in *Proc. 24th Int. Symp. Discharges Electr. Insul. Vacuum*, Sep. 2010, pp. 355–358.

[18] S. Jia, L. Zhang, L. Wang, B. Chen, Z. Shi, and W. Sun, "Numerical simulation of high-current vacuum arcs under axial magnetic fields with consideration of current density distribution at cathode," *IEEE Trans. Plasma Sci.*, vol. 39, no. 11, pp. 3233–3243, Nov. 2011.

[19] N. Wenzel, S. Kosse, A. Lawall, R. Renz, and W. Hartmann, "Numerical simulation of multi-component arcs in high-current vacuum interrupters," in *Proc. 25rd Int. Symp. Discharges Electr. Insul. Vacuum*, Sep. 2012, pp. 321–324.

[20] H. Hess, "The vacuum arc spot—A high pressure phenomenon," *J Phys. D, Appl. Phys.*, vol. 24, no. 1, pp. 36–40, 1991.

[21] D. L. Shmelev and E. A. Litvinov, "The computer simulation of the vacuum arc emission center," *IEEE Trans. Plasma Sci.*, vol. 25, no. 4, pp. 533–537, Aug. 1997.

[22] D. L. Shmelev and E. A. Litvinov, "Computer simulation of ecton in a vacuum arc," *IEEE Trans. Dielectr. Electr. Insul.*, vol. 6, no. 4, pp. 441–444, Aug. 1999.

[23] M. S. Benilov, "Understanding and modelling plasma-electrode interaction in high-pressure arc discharges: A review," *J. Phys. D, Appl. Phys.*, vol. 41, no. 14, pp. 144001-1–144001-30, Jul. 2008.

[24] F. Cayla, P. Freton, and J.-J. Gonzalez, "Arc/cathode interaction model," *IEEE Trans. Plasma Sci.*, vol. 36, no. 4, pp. 1944–1954, Aug. 2008.

[25] A. Bergner, M. Westermeier, C. Ruhrmann, P. Awakowicz, and J. Mentel, "Temperature measurements at thoriated tungsten electrodes in a model lamp and their interpretation by numerical simulation," *J. Phys. D, Appl. Phys.*, vol. 44, no. 50, pp. 505203-1–505203-3, Dec. 2011.

[26] I. I. Beilis, "Analysis of the cathode spot in a vacuum arc," *Sov. Phys. Tech. Phys.*, vol. 19, no. 2, pp. 251–256, 1974.

[27] V. A. Nemchinskii, "Theory of the vacuum arc," *Sov. Phys. Tech. Phys.*, vol. 24, no. 7, pp. 764–771, 1979.

[28] J. Prock, "Time-dependent description of cathode crater formation in vacuum arcs," *IEEE Trans. Plasma Sci.*, vol. 14, no. 4, pp. 482–491, Aug. 1986.

[29] J. Mitterauer and P. Till, "Computer simulation of the dynamics of plasma-surface interactions in vacuum arc cathode spots," *IEEE Trans. Plasma Sci.*, vol. 15, no. 5, pp. 488–501, Oct. 1987.

[30] E. Hantzsche, "Theoretical models of the cathode spot in arc discharges," *Contrib. Plasma Phys.*, vol. 32, no. 2, pp. 109–169, 1992,

[31] M. S. Benilov, "Nonlinear heat structures and arc-discharge electrode spots," *Phys. Rev. E*, vol. 48, no. 1, pp. 506–515, 1993.

[32] T. Klein, J. Paulini, and G. Simon, "Time-resolved description of cathode spot development in vacuum arcs," *J. Phys. D, Appl. Phys.*, vol. 27, no. 9, pp. 1914–1921, 1994.

[33] E. Hantzsche, "Theories of cathode spots," in *Handbook of Vacuum Arc Science and Technology: Fundamentals and Applications*, R. L. Boxman, D. M. Sanders, and P. J. Martin, Eds. Park Ridge, NJ, USA: Noyes, 1995, pp. 151–208.

[34] I. Beilis, "Theoretical modeling of cathode spot phenomena," in *Handbook of Vacuum Arc Science and Technology: Fundamentals and Applications*, R. L. Boxman, D. M. Sanders, and P. J. Martin, Eds. Park Ridge, NJ, USA: Noyes, 1995, pp. 208–256.

[35] Z.-J. He and R. Haug, "Cathode spot initiation in different external conditions," *J. Phys. D, Appl. Phys.*, vol. 30, no. 4, pp. 603–613, Feb. 1997.

[36] R. Schmoll, "Analysis of the interaction of cathode microprotrusions with low-temperature plasmas," *J. Phys. D, Appl. Phys.*, vol. 31, no. 15, pp. 1841–1851, Aug. 1998.

[37] I. I. Beilis, "State of the theory of vacuum arcs," *IEEE Trans. Plasma Sci.*, vol. 29, no. 5, pp. 657–670, Oct. 2001.

[38] I. V. Uimanov, "A two-dimensional nonstationary model of the initiation of an explosive center beneath the plasma of a vacuum arc cathode spot," *IEEE Trans. Plasma Sci.*, vol. 31, no. 5, pp. 822–826, Oct. 2003.

[39] S. A. Barengolts, G. A. Mesyats, and M. M. Tsventoukh, "Initiation of ecton processes by interaction of a plasma with a microprotrusion on a metal surface," *J. Experim. Theoretical Phys.*, vol. 107, no. 6, pp. 1039–1048, Dec. 2008.

[40] S. A. Barengolts, G. A. Mesyats, and M. M. Tsventoukh, "Ignition and sustainment of the explosive electron emission cyclic pulses—Ectons by plasma-surface interaction," in *Proc. 25rd Int. Symp. Discharges Electr. Insul. Vacuum*, Sep. 2012, pp. 376–379.

[41] N. A. Almeida, M. S. Benilov, and G. V. Naidis, "Unified modelling of near-cathode plasma layers in high-pressure arc discharges," *J. Phys. D, Appl. Phys.*, vol. 41, no. 24, pp. 245201-1–245201-26, Dec. 2008.

[42] V. A. Nemchinskii, "Monte-Carlo calculation of the erosion rate and ion current at a vacuum arc cathode," *Sov. Phys. Tech. Phys.*, vol. 27, no. 9, pp. 1073–1077, 1982.

[43] P. Chapelle, J. P. Bellot, A. Jardy, and D. Ablitzer, "Use of kinetic simulations for the determination of particle and energy fluxes at the cathode surface of a vacuum arc," *Eur. Phys. J. Appl. Phys.*, vol. 34, no. 1, pp. 43–53, Apr. 2006.

[44] D. L. Shmelev and T. Delachaux, "Computational model of the cathode attachment zone of constricted high current vacuum arcs," in *24th Int. Symp. Discharges Electr. Insul. Vacuum*, Sep. 2010, pp. 399–402.

[45] H. Timko, K. Matyash, R. Schneider, F. Djurabekova, K. Nordlund, A. Hansen, A. Descoeudres, J. Kovermann, A. Grudiev, W. Wuensch, S. Calatroni, and M. Taborelli, "A one-dimensional particle-in-cell model of plasma build-up in vacuum arcs," *Contr. Plasma Phys.*, vol. 51, no. 1, pp. 5–21, Jan. 2011.

[46] A. Anders, *Cathodic Arcs: From Fractal Spots to Energetic Condensation* (Springer Series on Atomic, Optical, and Plasma Physics). New York, NY, USA: Springer-Verlag, 2008.

[47] G. Ecker, "Theoretical aspects of the vacuum arc," in *Vacuum Arcs: Theory and Application*, J. M. Lafferty, Ed. New York, NY, USA: Wiley, 1980, pp. 228–320.

[48] M. S. Benilov, "Space-charge sheath with ions accelerated into the plasma," *J. Phys. D, Appl. Phys.*, vol. 43, no. 17, pp. 175203-1–175203-6, May 2010.

[49] A. V. Bolotov, A. V. Kozyrev, and Y. D. Korolev, "Model for the cathode layer of vacuum arc at nonmonotonical distribution of a potential in a near-cathode plasma," *Fizika Plasmy*, vol. 19, no. 5, pp. 709–719, 1993.

[50] A. Bolotov, A. Kozyrev, and Y. Korolev, "A physical model of the low-current-density vacuum arc," *IEEE Trans. Plasma Sci.*, vol. 23, no. 6, pp. 884–892, Dec. 1995.

[51] M. S. Benilov and L. G. Benilova, "The double sheath on cathodes of discharges burning in cathode vapour," *J. Phys. D, Appl. Phys.*, vol. 43, no. 34, pp. 345204-1–345204-12, Sep. 2010.

[52] M. S. Benilov and M. D. Cunha, "Heating of refractory cathodes by high-pressure arc plasmas: II," *J. Phys. D, Appl. Phys.*, vol. 36, no. 6, pp. 603–614, Mar. 2003.

[53] M. S. Benilov, "Maxwell's construction for non-linear heat structures and determination of radius of arc spots on cathodes," *Phys. Scripta*, vol. 58, no. 4, pp. 383–386, Mar. 1998.

[54] M. S. Benilov, "Method of matched asymptotic expansions versus intuitive approaches: Calculation of arc cathode spots," *IEEE Trans. Plasma Sci.*, vol. 32, no. 1, pp. 249–255, Feb. 2004.

[55] M. S. Benilov, M. D. Cunha, W. Hartmann, S. Kosse, A. Lawall, and N. Wenzel, "Space-resolved modeling of stationary spots on copper vacuum arc cathodes and on composite CuCr cathodes with large grains," *IEEE Trans. Plasma Sci.*, vol. 41, no. 8, pp. 1950–1958, Aug. 2013.

[56] L. M. Biberman, V. S. Vorob'ev, and I. T. Yakubov, *Kinetics of Nonequilibrium Low-Temperature Plasma*. New York, NY, USA: Plenum, 1987.

[57] M. Mitchner and C. H. Kruger, *Partially Ionized Gases*. New York, NY, USA: Wiley, 1973.

[58] M. S. Benilov, "The Child–Langmuir law and analytical theory of collisionless to collision-dominated sheaths," *Plasma Sour. Sci. Technol.*, vol. 18, no. 1, pp. 014005-1–014005-14, Feb. 2009.

[59] D. R. Lide, *CRC Handbook of Chemistry and Physics*, 84th ed. Boca Raton, FL, USA: CRC Press, 2004.
[60] W. F. Gale and T. C. Totemeier, Eds., *Smithells Metals Reference Book*, 8th ed. Amsterdam, The Netherlands: Elsevier, 2004.
[61] E. L. Murphy and R. H. Good, "Thermionic emission, field emission, and the transition region," *Phys. Rev.*, vol. 102, no. 6, pp. 1464–1473, 1956.
[62] M. S. Benilov and L. G. Benilova, "Field to thermo-field to thermionic electron emission: A practical guide to evaluation, effect on arc cathodes," in *Proc. ICPIG*, Jul. 2013.
[63] J. Paulini, T. Klein, and G. Simon, "Thermo-field emission and the Nottingham effect," *J. Phys. D, Appl. Phys.*, vol. 26, no. 8, pp. 1310–1315, Aug. 1993.
[64] G. S. Voronov, "A practical fit formula for ionization rate coefficients of atoms and ions by electron impact: Z=1–28," *Atomic Data Nucl. Data Tables*, vol. 65, no. 1, pp. 1–35, 1997.
[65] M. S. Benilov and G. V. Naidis, "Ionization layer at the edge of a fully ionized plasma," *Phys. Rev. E*, vol. 57, no. 2, pp. 2230–2241, 1998.
[66] W. Lotz, "Electron-impact ionization cross-sections for atoms up to z=108," *Z. Physik*, vol. 232, no. 2, pp. 101–107, 1970.
[67] H. S. Carslaw and J. C. Jaeger, *Conduction of Heat in Solids*. Oxford, U.K.: Clarendon, 1959.
[68] B. Jüttner, "Cathode spots of electric arcs," *J. Phys. D, Appl. Phys.*, vol. 34, no. 17, pp. 103–123, Sep. 2001.
[69] W. Hartmann, A. Lawall, R. Renz, N. Wenzel, and W. Wietzorek, "Experimental investigations on cathode spots and dynamical vacuum arc structure in an axial magnetic field," in *Proc. 23rd Int. Symp. Discharges Electr. Insul. Vacuum*, vol. 1. Sep. 2008, pp. 259–263.
[70] W. Hartmann, A. Lawall, R. Renz, N. Wenzel, and W. Wietzorek, "Cathode spots and arc structure in a dense, axial magnetic field-stabilised vacuum arc," in *Proc. 24th Int. Symp. Discharges Electr. Insul. Vacuum*, Sep. 2010, pp. 245–248.
[71] W. Hartmann, A. Lawall, R. Renz, M. Romheld, N. Wenzel, and W. Wietzorek, "Cathode spot dynamics and arc structure in a dense axial magnetic-field-stabilized vacuum arc," *IEEE Trans. Plasma Sci.*, vol. 39, no. 6, pp. 1324–1329, Jun. 2011.

Nelson A. Almeida was born in Coimbra, Portugal, in 1978. He received the B.Sc. degree in physics in 2000 and the the Ph.D. degree in 2009 from the University of Madeira, Madeira, Portugal.

His current research interests include near-electrode phenomena in high-pressure arc discharges. He has been with the University of Madeira, Funchal, Portugal, since 2000, as a Teaching Assistant, and since 2009, as an Assistant Professor.

Mikhail S. Benilov received the Diploma degree (Hons.) and the C.Sc. (Ph.D.) degree in physics from the Moscow Institute for Physics and Technology, Moscow, Russia, in 1974 and 1978, respectively, and the Doctor of Physical and Mathematical Sciences degree from the Institute for High Temperatures, USSR Academy of Sciences, Moscow, in 1990. His thesis focuses on theory of electrostatic probes and electrodes in high-pressure flowing plasmas.

He had been with the Institute for High Temperatures, USSR Academy of Sciences, Moscow, where he led a group working in plasma and nonlinear physics, numerical modeling, and fluid dynamics, after completing postgraduate courses with the Moscow Institute for Physics and Technology and Institute for Mechanics of Lomonosov Moscow State University, Moscow, in 1977. Since 1993, he has been a Professor and a Chair with the Department of Physics, University of Madeira. His current research interests include plasma physics, in particular, plasma-electrode interaction, nonlinear physics, and numerical modeling.

Dr. Benilov received the Alexander von Humboldt Research Fellowship in 1990 and stayed for two years with the Ruhr-Universität Bochum, Germany, working on the theory and simulation of near-electrode phenomena.

Larissa G. Benilova received the Diploma degree in electrical engineering from the Moscow Institute of Railway Engineering, Moscow, Russia.

She was employed at several computing centers in Moscow and Bochum, Germany, from 1975 to 1996. From 1997 to 1999, she collaborated as an Engineer-Programmer with Instituto Superior Técnico, Lisbon, Portugal. Since 2001, she has been contracted by Universidade da Madeira, Funchal, Portugal, as an Engineer-Programmer, and has performed scientific programming and numerical simulations in the framework of a number of research projects in plasma science and applications funded by European Union, Fundação para a Ciência e a Tecnologia of Portugal, and by the industries.

Werner Hartmann received the M.S. degree in physics in 1981 from the University of Erlangen, Erlangen, Germany, where he received the Ph.D. degree in 1986.

He has been with Siemens Corporate Technology, as a Researcher, Research Group Leader, Project Manager, and as a Program Manager, since 1991. He was a Research and Teaching Assistant with the University of Erlangen, Physics Department, from 1986 to 1991, and with the University of Southern California, Los Angeles, CA, USA, in 1987 and 1988, where he conducted research on cold cathode thyratrons/pseudosparks and fast dynamic z-pinches as EUV light sources. He was responsible for fundamental and applied research into vacuum switching arc physics and devices at the Corporate Technology of Siemens, being involved in the development of low voltage contactors, low voltage circuit breakers up to 130 kA breaking capacity, medium voltage vacuum circuit breakers, and the successful development of high voltage vacuum circuit breakers for 72 and 145 kV. He was involved in the development of a fully 3-D, fully transient software code for the simulation of low voltage switching arcs in air as a Project Manager. He developed environmental and environmentally friendly technologies for industrial applications, mainly in the areas of clean water, clean air, and electroporation. Since 2006, his research interests have been in the field of mining applications, particularly in the field of flotation and magnetic separation. Currently, he holds the position of a Senior Key Expert in the area of environmental technologies.

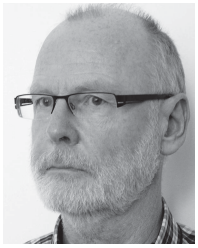

Norbert Wenzel received the M.Ed. degree in physics and mathematics from the University of Heidelberg, Heidelberg, Germany, in 1979, and the Ph.D. degree in physics with the same institution in 1985.

He has been with Siemens Corporate Technology as a Researcher, Test Laboratory Head, Project Leader, and as a Radiation Protection Officer since 1985. From 1978 to 1985, he was a Research and Teaching Assistant with the University of Heidelberg, Department of Applied Physics, and with the Institute of Plasma Research, University of Stuttgart, Stuttgart, Germany, on fusion-oriented plasma physics and plasma diagnostics. In 1982, he held a EURATOM fellowship with the Nuclear Fusion Research Center of the Association ENEA in Frascati, Rome, Italy. From 1985 to 1992, he applied nonlinear Raman spectroscopic techniques to industrial processes, such as low voltage air breakers and gas lasers. He was responsible for the development of sealed-off carbon dioxide slab lasers excited by radio-waves and microwaves. Since 1992, he has been working in the field of fundamental and applied research of switching arcs with the Corporate Technology of Siemens. As the Head of a Synthetic Test Laboratory, he was involved in the development of low and medium voltage vacuum interrupters up to 130 kA breaking capacity and the development of high voltage vacuum circuit breakers for 72 and 145 kV. Since 2006, he has been extending his field of activities to the physical modeling and numerical simulation of arc plasmas taking into account cathode surface phenomena. He developed a transient, 3-D simulation software to describe the evolution of vacuum switching arcs in axial magnetic field contacts. Currently, he holds the position of Senior Key Expert Research Scientist in the area of switching technologies.